



Cite this: *J. Mater. Chem. A*, 2014, 2, 15722

Received 28th June 2014  
Accepted 6th August 2014

DOI: 10.1039/c4ta03308f

[www.rsc.org/MaterialsA](http://www.rsc.org/MaterialsA)

Layered zeolite precursor MCM-22P can be stabilized as interlayer expanded structure MWW-IEZ with enlarged pores by silylation producing  $-\text{O}-\text{Si}(\text{OH})_2-\text{O}-$  bridges. It adsorbs two times more cerium than MCM-22 and becomes activated for CO oxidation to  $\text{CO}_2$  at room temperature. This represents one of the most notable activity enhancements upon modification of layered zeolites.

Zeolites are valuable catalytic materials<sup>1</sup> widely used in industrial processes<sup>2</sup> with exceptional activity and selectivity produced by their framework structures with ordered micropores and strong acid sites resulting from Al incorporation.<sup>3,4</sup> These inherent zeolite characteristics can be further expanded and enhanced by modification with metal ions as exemplified by the lanthanide stabilization of zeolite Y making it a superb cracking catalyst<sup>5</sup> and Ti-ZSM-5, which is very active for oxidations.<sup>6</sup> However, the very qualities that make zeolites exceptional, *i.e.* rigid frameworks with fixed micropores, often prevent their functionalization with transition metals because of size constraints or charge incompatibility. New opportunities appeared with the discovery of zeolite framework formation as layered materials.<sup>7</sup> It enabled spatial modification,<sup>8</sup> especially expansion, similar to the well known behavior of 2D solids.<sup>9-12</sup> As shown below, structural expansion can produce new results, which may be prohibited by the rigidity of 3D frameworks, by combining zeolitic activity with new metal functionality. The field of layered, 2D zeolites<sup>13</sup> is expanding<sup>14</sup> including remarkable findings like the first top down synthesis of a new zeolite<sup>15</sup> and preparation of ZSM-5 as nanosheets by design.<sup>16</sup> The title zeolite of this work MCM-22, with the framework denoted

## Activity enhancement of zeolite MCM-22 by interlayer expansion enabling higher Ce loading and room temperature CO oxidation†

Wiesław J. Roth,<sup>a</sup> Waclaw Makowski,<sup>a</sup> Bartosz Marszałek,<sup>a</sup> Piotr Michorczyk,<sup>b</sup> Weronika Skuza<sup>a</sup> and Barbara Gil<sup>\*a</sup>

MWW, is the archetype and leading representative of 2D zeolites. Its layers contain internal 10-ring sinusoidal channels and 12-ring cavities on the surface. The latter form  $0.7 \times 1.8$  nm supercages accessible through elliptical 10-ring apertures in the 3D framework MCM-22.<sup>7</sup> Expansion of the interlayer distance increases access to these surface cavities containing Brønsted acid sites. MCM-22 is a commercial catalyst for aromatic alkylation with exceptional selectivity attributed to its surface cavities.<sup>17</sup> More than ten frameworks demonstrated formation of layered forms<sup>18</sup> and their ranks continue to grow.<sup>11,19</sup> Many more,<sup>20</sup> possibly all zeolites<sup>9</sup> may allow formation of 2D species.

The precursor MCM-22P contracts upon calcination producing the complete MWW framework but it can be stabilized as expanded zeolite by silylation<sup>21</sup> with insertion of  $\text{O}_2\text{Si}(\text{OH})_2$  interlayer bridges. The product, called interlayer expanded zeolite, MWW-IEZ, has 12-ring openings between layers.<sup>22</sup> It is shown here to allow increased adsorption of  $\text{Ce}^{3+}$  with generation of new activity – CO oxidation at room temperature (RT), which has been monitored quantitatively by IR. The standard 3D MCM-22 has much lower capacity for Ce and is inactive showing no CO adsorption at RT. The observed activation seems to be related to increased Ce access to Al centers and generation of metal species in the formal 4+ state.

The oxidation of CO is currently of great interest because of the desire and mandates to remove toxic components from exhaust gases. Many metal<sup>23</sup> and oxide catalysts<sup>24</sup> are active for this process. Gold nanoparticles are very active at low temperatures and better than platinum metals.<sup>23</sup> Recent examples of active materials include cerium/cearia with noble metals<sup>25,26</sup> and ZSM-5,<sup>27,28</sup> Zn in ZSM-5,<sup>29</sup> rare earth in MCM-41<sup>30</sup> and ceria hollow nano-spheres.<sup>31</sup> Rare earth incorporation into zeolites provided the first breakthrough in zeolite catalysis<sup>5</sup> but proved problematic with important medium pore high silica zeolites. The present result with MWW-IEZ demonstrates that expansion of zeolite structures may enhance incorporation of metal ions and expand catalytic potential, especially oxidation, which for zeolites is still below expectations.

<sup>a</sup>Faculty of Chemistry, Jagiellonian University in Kraków, Ingardena 3, 30-060 Kraków, Poland. E-mail: [gil@chemia.uj.edu.pl](mailto:gil@chemia.uj.edu.pl); Fax: +48 12 634 0515

<sup>b</sup>Faculty of Chemical Engineering and Technology, Cracow University of Technology, Warszawska 24, 31-155 Kraków, Poland

† Electronic supplementary information (ESI) available: Details of experiments,  $\text{H}_2\text{TPR}$  profiles, CO adsorption on La-MWW and enlarged versions of XRD patterns with MWW zeolites before cerium-exchange. See DOI: [10.1039/c4ta03308f](https://doi.org/10.1039/c4ta03308f)



## Results and discussion

Detailed description of experimental procedures is provided in the ESI.† MCM-22P and MCM-56/49 were prepared using gels with Si/Al = 24 and 12, respectively. MCM-22P was silylated with  $\text{CH}_3\text{Si}(\text{OCH}_2\text{CH}_3)_2$ . The XRD,  $\text{N}_2$  sorption and spectroscopic characterizations were based on standard procedures.

Three MWW materials were investigated in calcined forms: the standard MCM-22 zeolite ( $\text{Si/Al}_{\text{gel}} = 24$ ), its IEZ derivative with discrete  $\text{O}_2\text{Si}(\text{OH})_2$  interlayer bridges, and high Al MCM-56/49 ( $\text{Si/Al}_{\text{gel}} = 12$ ) containing randomly packed MWW layers with some 3D ordering concluded from XRD. The identity and good quality of materials were confirmed by XRD and  $\text{N}_2$  sorption (Fig. 1 and 2). MWW-IEZ showed a distinct peak at  $6.4^\circ$  in XRD, proving an interlayer distance of 2.7 nm and increased micropore volume due to the expanded structure. For MWW-IEZ the  $\text{N}_2$  adsorption isotherm shows a considerable slope at intermediate pressures indicating increased access to the interlayer space, *i.e.* the external surface of the layers. Basic composition and acidity properties are listed in Table 1.

The pyridine adsorption measured by FTIR indicated high Brønsted acid site concentrations (BAS) of over  $600 \mu\text{mol g}^{-1}$ , consistent with previously reported data.<sup>32</sup> The unmodified zeolites MCM-22 and MCM-56/49 showed a slight increase of the BAS after incorporation of  $\text{Ce}^{3+}$ .

The expanded IEZ form adsorbed 2 times more cerium ions with about the same Al content as MCM-22. A significant reduction in the BAS ensued. The enhanced Ce adsorption must be related to the expanded interlayer distance, which appears to allow diffusion of ions between the layers. The incorporation of Ce into high silica zeolites ( $\text{Si/Al} > 5$ ) cannot occur by the standard balancing of the 3+ or 4+ charge by 3 to 4 Al centers, which are unlikely to be grouped close enough. The overall effective charge on such ions may be reduced<sup>33</sup> through interactions with the oxide lattice, proton losses from coordinated water and other not fully accounted for phenomena.

The XRD patterns show the absence of either  $\text{CeO}_2$  or  $\text{Ce}_2\text{O}_3$  oxides suggesting that the sizes of postulated oxide-like clusters are below the detection limit for this method.

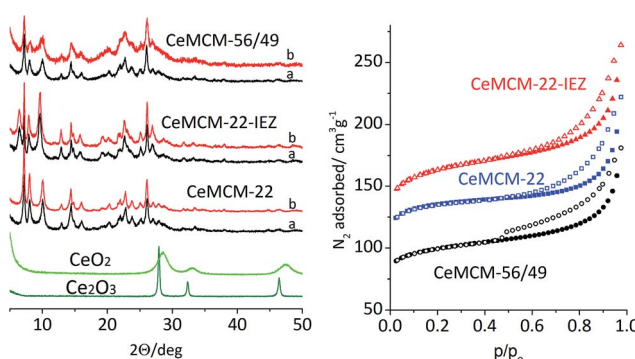


Fig. 1 XRD for  $\text{CeO}_2$ ,  $\text{Ce}_2\text{O}_3$  and Ce-MCM-22, Ce-MCM-22-IEZ, and Ce-MCM-56/49 zeolites, (a) calcined and cerium-exchanged, (b) cerium-exchanged and vacuum activated samples;  $\text{N}_2$  isotherms for calcined samples.

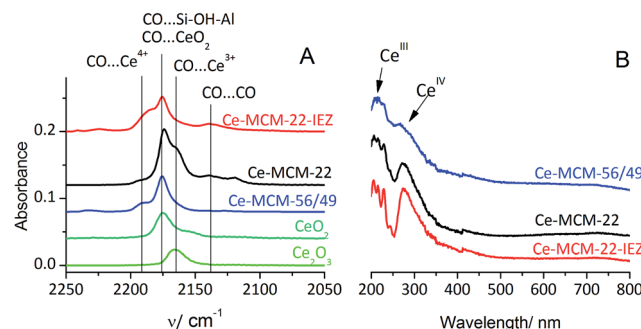


Fig. 2 (A) IR spectra of CO adsorbed at  $-100^\circ\text{C}$  on cerium-zeolites, commercial  $\text{Ce}_2\text{O}_3$  and  $\text{CeO}_2$ . (B) UV-Vis-DRS spectra of cerium-zeolites.

The nature of incorporated Ce was established by IR after CO adsorption at low temperature ( $-100^\circ\text{C}$ ). The spectra, shown in Fig. 2A, indicated only  $\text{Ce}^{3+}$  species in the MCM-22 zeolite while MCM-56 and MWW-IEZ contained Ce in both 3+ and 4+ oxidation states in different proportions.  $\text{Ce}^{4+}$  enables oxidation of CO as temperature increases. In all cases, the band at  $2175 \text{ cm}^{-1}$  due to CO on OH groups is present. CO adsorbed on MCM-22 reveals a shoulder at  $2165 \text{ cm}^{-1}$ , the same as when adsorbed on bulk  $\text{Ce}_2\text{O}_3$ . It suggests that most of the Ce is located at the external surfaces of the zeolite crystals, in the form of small  $\text{Ce}_2\text{O}_3$ -like clusters. The Ce-MCM-22-IEZ and Ce-MCM-56/49 show an additional IR band at  $2190 \text{ cm}^{-1}$ , which can be assigned<sup>34</sup> to CO adsorbed on  $\text{Ce}^{4+}$ . The position is at higher frequency than in commercial  $\text{CeO}_2$  ( $2175 \text{ cm}^{-1}$ ) suggesting greater coordinative unsaturation of  $\text{Ce}^{4+}$ .<sup>35</sup>

The increasing adsorption of Ce ions, apparently caused by a greater number of Al sites accessible to them in different MWW forms, results in increasing oxidation to  $\text{Ce}^{4+}$  and activation of CO. MCM-56/49 is more open than MCM-22 and has a higher Al content, which is presumably conducive to generation of  $\text{Ce}^{4+}$  centers that retain adsorbed CO and cause its oxidation. For Ce-MCM-22-IEZ the share of  $\text{Ce}^{4+}$  is the highest, probably because the increased separation of the zeolite layers produces enough room for the  $\text{Ce}^{4+}$  cations to be located in exchangeable positions replacing some acidic protons.

This is suggested by the decreased concentration of BAS. Most likely some small  $\text{CeO}_2$ -like clusters are formed at the surface of MWW layers, both internal in the crystal and external, including surface pockets. The geminal silanols in the interlayer bridges appear unchanged and do not interact with cerium.

The proposed nature of Ce centers on MWW zeolites was supported by UV-Vis spectra (Fig. 2B), which indicated the presence of small clusters of oxygen-coordinated  $\text{Ce}^{4+}$  and  $\text{Ce}^{3+}$  ions. A band near  $300 \text{ nm}$  is due to  $\text{Ce}^{IV}$ ,<sup>36</sup> while the band below  $260 \text{ nm}$  is assigned to  $\text{Ce}^{III}$ . Both are very sensitive to the environment and dispersion of Ce ions.<sup>37</sup>

The oxidation of CO was observed upon warming of the IR cell to RT, after the initial adsorption at  $-100^\circ\text{C}$  and desorption of excess gas. The band for CO interacting with  $\text{Ce}^{4+}$  cations decreased with time, and the adsorbed  $\text{CO}_2$  band ( $2360 \text{ cm}^{-1}$ )



Table 1 Basic properties of the studied materials

Zeolite	Si/Al, XRF	BET, $\text{m}^2 \text{g}^{-1}$	Ce (La), wt%	BAS $\mu\text{mol g}^{-1}$	LAS, $\mu\text{mol g}^{-1}$
MCM-22	13	436	—	664	46
MCM-22-IEZ	13	531	—	621	112
MCM-56/49	8	324	—	678	56
Ce-MCM-22	13	—	0.40	714	95
Ce-MCM-22-IEZ	13	—	0.88	357	70
Ce-MCM-56/49	8	—	0.74	792	72
La-MCM-22	12	—	0.28	721	84
La-MCM-22-IEZ	13	—	0.52	457	110
La-MCM-56/49	7	—	0.45	963	48

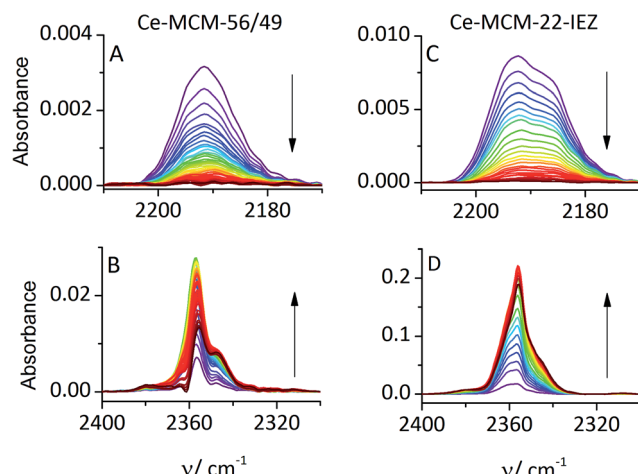


Fig. 3 IR spectra recorded every 15 min in the CO (A and C) and  $\text{CO}_2$  region (B and D) for Ce-MCM-56/49 (A and B) and Ce-MCM-22-IEZ (C and D). (Note differences in intensities between upper and lower plots.)

increased, as shown in Fig. 3. Ce-MCM-22 did not show adsorbed CO at RT indicating an insufficient content of  $\text{Ce}^{4+}$  for detectable reaction. Both Ce-MCM-22-IEZ and Ce-MCM-56/49 showed oxidation of CO, attributed to the presence of  $\text{Ce}^{4+}$ . The expanded IEZ structure was more active, which reflects its higher content of  $\text{Ce}^{4+}$ .

The participation of  $\text{Ce}^{4+}$  is supported by control studies with La-MWW materials, where  $3+$  to  $4+$  metal oxidation is not viable. Only La-MCM-22-IEZ shows significant uptake of CO at  $-100^\circ\text{C}$  but no CO is retained at RT and consequently no

oxidation is taking place (cf. ESI†). These results are important in supporting the critical role of redox metal centers represented by Ce in contrast to La.

The restoration of  $\text{Ce}^{4+}$  was demonstrated for Ce-MCM-22-IEZ. After evacuation of  $\text{CO}_2$  at RT the temperature was lowered to  $-100^\circ\text{C}$  but new exposure to CO did not restore the  $\text{Ce}^{4+}$ -CO band at  $2190 \text{ cm}^{-1}$ . This confirms that reduction to  $\text{Ce}^{3+}$  occurred upon CO oxidation at RT. When the sample was activated in pure oxygen (40 min,  $450^\circ\text{C}$ ) and the adsorption of CO was repeated at  $-100^\circ\text{C}$ , the band  $2190 \text{ cm}^{-1}$  ( $\text{CO-Ce}^{4+}$ ) was restored to its original intensity (Fig. 4). This demonstrates potential for the catalytic process, which has been confirmed by preliminary studies.

## Conclusions

The reported results confirm that layered zeolite materials provide new opportunities because of potential for post-synthesis modification. The expansion of the interlayer space enabled increased adsorption of larger metal cations, such as Ce, resulting in novel enhanced activity. The approach may be general and can be expanded to other active metals and processes. MCM-22 is particularly attractive because of convenient availability in diverse active forms.

## Acknowledgements

This work was financed with the funds from the Narodowe Centrum Nauki provided on the basis of decision number DEC-2011/03/B/ST5/01551. The IR measurements were carried out with the equipment purchased thanks to the financial support of the European Regional Development Fund in the framework of the Polish Innovation Economy Operational Program (contract no. POIG.02.01.00-12-023/08).

## Notes and references

- 1 A. F. Masters and T. Maschmeyer, *Microporous Mesoporous Mater.*, 2011, **142**, 423–438.
- 2 I. Fechete, Y. Wang and J. C. Védrine, *Catal. Today*, 2012, **189**, 2–27.

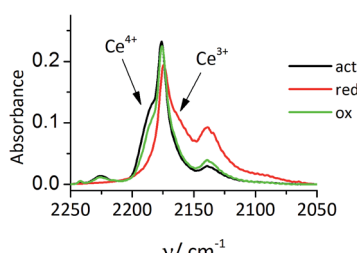


Fig. 4 IR spectra of CO adsorbed at  $-100^\circ\text{C}$  on activation, reduced by CO reaction and oxidized Ce-MCM-22-IEZ.



3 C. Baerlocher, L. B. McCusker and D. H. Olson, *Atlas of Zeolite Framework Types*, Elsevier, Amsterdam, 2007, <http://www.iza-structure.org>.

4 J. Čejka, H. van Bekkum, A. Corma and F. Schueth, *Introduction to Zeolite Molecular Sieves*, Elsevier, Amsterdam, 2007.

5 C. J. Plank, E. J. Rosinski and W. P. Hawthorne, *Ind. Eng. Chem. Prod. Res. Dev.*, 1964, **3**, 165–169.

6 G. Bellussi and V. Fattore, *Stud. Surf. Sci. Catal.*, 1991, **69**, 79–92.

7 M. E. Leonowicz, J. A. Lawton, S. L. Lawton and M. K. Rubin, *Science*, 1994, **264**, 1910–1913.

8 W. J. Roth, C. T. Kresge, J. C. Vartuli, M. E. Leonowicz, A. S. Fung and S. B. McCullen, *Stud. Surf. Sci. Catal.*, 1995, **94**, 301–308.

9 W. J. Roth, *Stud. Surf. Sci. Catal.*, 2007, **168**, 221–239.

10 W. J. Roth and J. Čejka, *Catal. Sci. Technol.*, 2011, **1**, 43–53.

11 F. S. O. Ramos, M. K. De Pietre and H. O. Pastore, *RSC Adv.*, 2013, **3**, 2084–2111.

12 A. Corma, U. Diaz, M. E. Domine and V. Fornés, *Angew. Chem., Int. Ed.*, 2000, **39**, 1499–1501.

13 W. J. Roth and D. L. Dorset, *Microporous Mesoporous Mater.*, 2011, **142**, 32–36.

14 W. J. Roth, P. Nachtigall, R. E. Morris and J. Čejka, *Chem. Rev.*, 2014, **114**, 4807–4837.

15 W. J. Roth, P. Nachtigall, R. E. Morris, P. S. Wheatley, V. R. Seymour, S. E. Ashbrook, P. Chlubná, L. Grajciar, M. Položij, A. Zukal, O. Shvets and J. Čejka, *Nat. Chem.*, 2013, **5**, 628–633.

16 M. Choi, K. Na, J. Kim, Y. Sakamoto, O. Terasaki and R. Ryoo, *Nature*, 2009, **461**, 246–249.

17 T. F. Degnan Jr, C. M. Smith and C. R. Venkat, *Appl. Catal., A*, 2001, **221**, 283–294.

18 W. J. Roth, B. Gil and B. Marszalek, *Catal. Today*, 2014, **227**, 9–14.

19 B. Marler and H. Gies, *Eur. J. Mineral.*, 2012, **24**, 405–428.

20 K. Na, C. Jo, J. Kim, K. Cho, J. Jung, Y. Seo, R. J. Messinger, B. F. Chmelka and R. Ryoo, *Science*, 2011, **333**, 328–332.

21 P. Wu, J. F. Ruan, L. L. Wang, L. L. Wu, Y. Wang, Y. M. Liu, W. B. Fan, M. Y. He, O. Terasaki and T. Tatsumi, *J. Am. Chem. Soc.*, 2008, **130**, 8178–8187.

22 W. B. Fan, P. Wu, S. Namba and T. Tatsumi, *Angew. Chem., Int. Ed.*, 2004, **43**, 236–240.

23 Y. Yu, J. Huang, T. Ishida and M. Haruta, in *Modern Heterogeneous Oxidation Catalysis*, ed. N. Mizuno, Wiley, Weinheim, 2009.

24 S. Royer and D. Duprez, *ChemCatChem*, 2011, **3**, 24–65.

25 W. Han, P. Zhang, Z. Tang, X. Pan and G. Lu, *J. Sol-Gel Sci. Technol.*, 2013, **66**, 526–532.

26 S. Zeng, W. Zhang, M. Śliwa and H. Su, *Int. J. Hydrogen Energy*, 2013, **38**, 3597–3605.

27 W. Han, Z. Tang, P. Zhang and G. Lu, *Catal. Surv. Asia*, 2013, **17**, 147–155.

28 W. Han, P. Zhang, Z. Tang and G. Lu, *Process Saf. Environ. Prot.*, 2013, DOI: 10.1016/j.psep.2013.04.003.

29 G. Qi, J. Xu, J. Su, J. Chen, X. Wang and F. Deng, *J. Am. Chem. Soc.*, 2013, **135**, 6762–6765.

30 O. A. González Vargas, J. A. De Los Reyes Heredia, A. Montesinos Castellanos, L. F. Chen and J. A. Wang, *Mater. Chem. Phys.*, 2013, **139**, 125–133.

31 Y. Jiao, F. Wang, X. Ma, Q. Tang, K. Wang, Y. Guo and L. Yang, *Microporous Mesoporous Mater.*, 2013, **176**, 1–7.

32 B. Gil, W. Makowski, B. Marszalek, W. J. Roth, M. Kubu, J. Čejka and Z. Olejniczak, *J. Chem. Soc., Dalton Trans.*, 2014, **43**, 10501–10511.

33 B. Gil, P. Pietrzyk, J. Datka, P. Kozyra and Z. Sojka, *Stud. Surf. Sci. Catal.*, 2005, **158A**, 893–900.

34 A. Bensalem, F. Bozon-Verduraz, M. Delamar and G. Bugli, *Appl. Catal., A*, 1995, **121**, 81–93.

35 C. Binet, M. Daturi and J. C. Lavalley, *Catal. Today*, 1999, **50**, 207–225.

36 R. Si, Y. W. Zhang, L. P. You and C. H. Yan, *Angew. Chem., Int. Ed.*, 2005, **44**, 3256–3260.

37 A. Bensalem, J. C. Muller and F. Bozon-Verduraz, *J. Chem. Soc., Faraday Trans.*, 1992, **88**, 153–154.

